RSC Advances

COMMUNICATION

View Article Online
View Journal | View Issue

Cite this: *RSC Adv.*, 2014, **4**, 59114

Received 27th August 2014
Accepted 16th October 2014

DOI: 10.1039/c4ra09355k

www.rsc.org/advances

New facile synthesis of one-dimensional Ag@TiO_2 anatase core–shell nanowires for enhanced photocatalytic properties†

Qingsong Dong, Hongchao Yu, Zhengbo Jiao, Gongxuan Lu and Yingpu Bi*

One-dimensional Ag@TiO_2 anatase core–shell nanowires are fabricated through a hydrolysis reaction and subsequent thermal-induced method. This photocatalyst exhibits much higher photocatalytic activities than Ag nanowires and TiO_2 anatase nanoparticles under visible-light irradiation.

Anatase (TiO_2) has been extensively studied as a photocatalyst for various reactions due to its low cost, strong oxidizing power and nontoxic nature.[1–3] Its large band gap of 3.2 eV means its excited only by UV irradiation (only 4% of the total sunlight), which greatly limits its efficiency in the utilization of solar energy as well as practical applications. Therefore, TiO_2 requires an external bias to shift its absorption from the UV region into the visible-light region, allowing for more photons to be absorbed and utilized in the process of photocatalytic reaction. A large amount of progress has been made in the area of visible-light-active TiO_2 by doping metal elements into the TiO_2 lattice,[4–9] and deposition of noble metals on the TiO_2 surface.[10–17] These metal-modified TiO_2 nanomaterials displayed great potentials in photocatalytic and photoelectrochemical applications. However, doping or depositing metals on the TiO_2 results in the exposure of metals to the reactants and surrounding media, and the corrosion, dissolution and reaction of metals during the photocatalytic reaction limit the efficacy of photocatalysts, especially for long-term working.[18] It is therefore advantageous to have the core–shell architecture whereby the metals as core are protected from being oxidized.

In recent years, Ag@TiO_2 core–shell motif has attracted attention because silver nanomaterials display some unique activities in chemical and biological sensing, which are based on surface-enhanced Raman scattering, localized surface plasmon resonance, and metal-enhanced fluorescence. Among such nanocomposite structures, many Ag@TiO_2 core–shell nano-particles have been studied,[18–24] while the TiO_2 shells usually lead to particles aggregation, resulting in lower the active surface area. Some Ag@TiO_2 core–shell nanowires have also been reported. For instance, Jeong and co-workers prepared Ag@TiO_2 anatase open core–shell nanowires arrays *via* electrodeposition method.[25] Yu *et al.* prepared Ag@TiO_2 anatase core–shell composites (nanowires and nanorods) by vapor-thermal method.[26] Besides, two Ag@TiO_2 amorphous core–shell nanowires were respectively reported by Chin[27] and Han.[28] In this work, we prepared the highly dispersible, evenly coated core–shell type of photocatalyst, with Ag nanowires as the metal cores and TiO_2 anatase as the oxide shells. To the best of our knowledge, this is the first time that the hydrolysis preparation and visible-light photocatalytic activity of plasmonic photocatalyst Ag@TiO_2 anatase core–shell nanowires has been presented.‡

The morphologies of Ag@TiO_2 nanocomposites prepared by a hydrolysis reaction of tetrabutyl titanate on the Ag nanowires[29] were characterized by SEM. The SEM image (Fig. 1A) reveals that the obtained products with lengths of up to several tens of micrometers feature the core–shell nanostructures, due to the contrast difference between the diameter of 300 nm for the products and that of 100 nm for its precursor Ag nanowires. Furthermore, the corresponding XPS spectra provide structural information for the Ag@TiO_2 nanocomposites, as shown in Fig. 1B–D (the full XPS spectrum is shown Fig. S1†). It can be seen that the core–shell nanowires are mainly composed of Ti, Ag, and O elements. Ti 2p1/2 (464.1 eV) and Ti 2p3/2 (458.4 eV) peaks are shown in Fig. 1B, which are assigned to the Ti^{4+} oxidation state according to reported XPS data.[30] In Fig. 1D, the peaks observed at 368.1 and 374.1 eV can be respectively ascribed to Ag 3d3/2 and Ag 3d5/2 of the metallic silver,[31] and the 6.0 eV difference between the binding energy of Ag 3d5/2 and 3d3/2 peaks is also characteristic of metallic Ag 3d states.[32] Because the material of Ag@TiO_2 core–shell nanowires reported by us are not absolutely perfect, small parts of Ag

State Key Laboratory for Oxo-Synthesis & Selective Oxidation and National Engineering Research Center for Fine Petrochemical Intermediate, Lanzhou Institute of Chemical Physics, CAS, Lanzhou, 730000, China. E-mail: yingpubi@licp.cas.cn

† Electronic supplementary information (ESI) available: Characterization and additional figures. See DOI: 10.1039/c4ra09355k

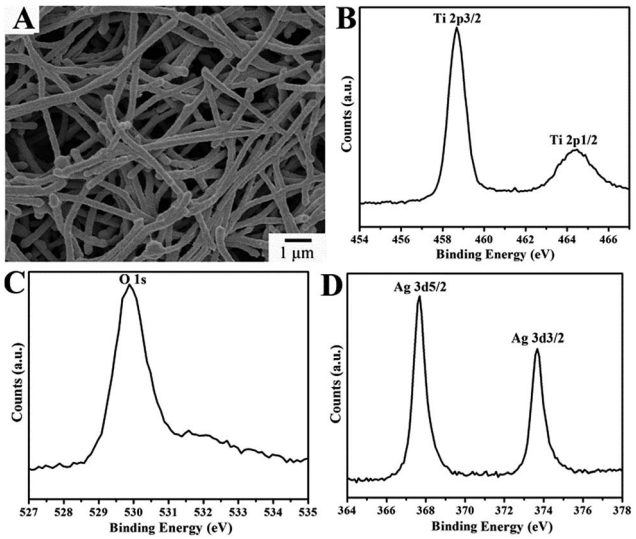

Fig. 1 (A) SEM images of Ag@TiO_2 core–shell nanowires prepared by hydrolysis reaction; XPS (B) Ti 2p peaks, (C) O 1s peak, and (D) Ag 3d peaks.

nanowires are exposed (Fig. S2†), so Ag signals can be shown in the XPS spectrum of the Ag@TiO_2 core–shell nanowires. While the XRD patterns of this products show that no TiO_2 diffraction peaks are observed (Fig. S3†), verifying that the TiO_2 shell is mainly amorphous (ref. 33).

Usually the amorphous TiO_2 can be transformed into anatase phase *via* hydrothermal reaction, so the Ag@TiO_2 nanowires prepared by hydrolyzing were further treated under hydrothermal condition at 160 °C for 24 h. Fig. 2A show typical SEM image of the Ag@TiO_2 nanoproducts that were obtained by hydrothermal process. It can be clearly seen from Fig. 2A that Ag@TiO_2 prepared by hydrolysis reaction and Ag@TiO_2 processed by hydrothermal reaction have a similar morphology and the thermal-induced system does not significantly influence the morphology of nanowires. Further observation indicates that the surface of the post-processing products is much rougher than that of the amorphous, implying that the former are composed of larger TiO_2 nanoparticles (the inset of Fig. 2A). To get more information about the nanowires, the Ag@TiO_2 nanowire was characterized by TEM, as shown in Fig. 2B. TEM image shows that the silver nanowires are encapsulated by a layer of TiO_2, and the thickness of the TiO_2 shell is about 100 nm. The anatase formation of TiO_2 can be confirmed by the XRD. Fig. 2C shows the XRD patterns of the Ag@TiO_2, pure anatase, and Ag. Compared with the XRD pattern of the Ag, that of Ag@TiO_2 obviously shows eight additional peaks, which are indexed to the anatase phase, indicating that anatase forms after hydrothermal process. Fig. 2D shows the UV-Vis absorption spectra of the TiO_2-amorphous, TiO_2-anatase and the as-synthesized Ag@TiO_2-anatase. It can be clearly seen that TiO_2-amorphous and TiO_2-anatase only shows strong absorption in the ultraviolet region with an absorption edge at 350 and 380 nm, respectively. While Ag@TiO_2-anatase exhibits a stronger absorption in both the ultraviolet and visible region due to the contribution of SPR of silver nanowires.

Furthermore, a potential reaction approach explaining the above growth process is identified and the schematic illustration is shown in Fig. 3A. In the Ag nanowire solution containing H_2O molecules, H_2O can be adsorbed on the surface of the silver nanowires because of O···Ag interaction. When TBT is introduced, part of TBT *in situ* hydrolyzes with the adsorbed water on the surface of the silver wires to form TiO_2 amorphous.

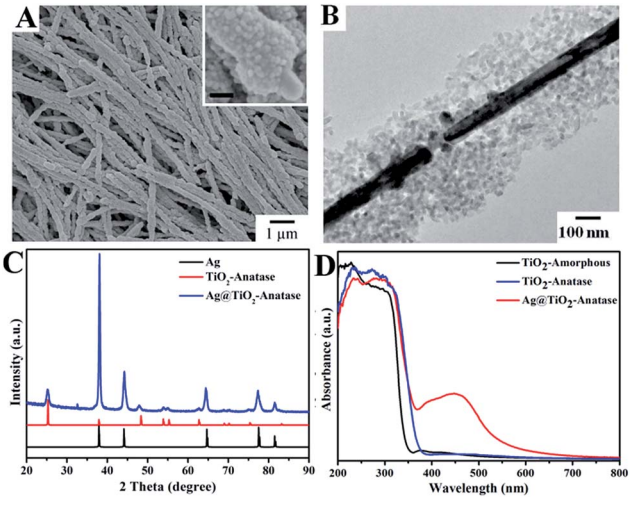

Fig. 2 (A) SEM images of Ag@TiO_2 core–shell nanowires prepared by hydrolysis reaction (inset scale bar = 150 nm); (B) TEM image of the core-shell nanowires; (C) XRD patterns of the Ag (black line), pure TiO_2-anatase (red line), and as-prepared Ag@TiO_2-anatase (blue line); and (D) UV-Vis absorption spectra of the TiO_2-amorphous (black line), TiO_2-anatase (blue line), and Ag@TiO_2-anatase (red line).

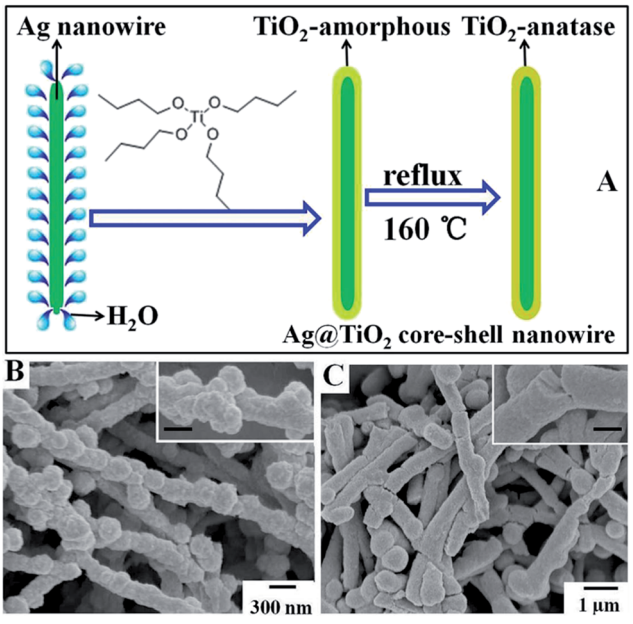

Fig. 3 (A) The possible growth process of TiO_2 nanoparticles to Ag nanowires; (B) SEM images of products prepared with 5 mL of H_2O (inset scale bar = 150 nm); (C) SEM images of products prepared with 4.0 g of TBT (inset scale bar = 400 nm).

Simultaneously, the other part of TBT hydrolyzes with free water to form amorphous TiO_2 coating onto the TiO_2 formed on the surface of the silver wires *via* a process known as Ostwald ripening.[34] Then, the amorphous TiO_2 is transformed into anatase phase *via* hydrothermal reaction at 160 °C. In addition, the influence of the amount of both H_2O and TBT on the structure and morphology of the composite nanowires has also been investigated. As shown in Fig. 3B, when H_2O in this reaction system increased to 5 mL, the surface of the Ag@TiO_2 nanowires became quite rough and large TiO_2 nanoparticles appeared on their surface as compared with the Ag@TiO_2 prepared with 3 mL H_2O (Fig. 1A). When the amount of TBT was increased to 4.0 g, the morphology of the as-prepared Ag@TiO_2 becomes one-dimensional short rods rather than nanowires (Fig. 3C). Therefore, it can be concluded that the amounts of H_2O and TBT plays an important role in determining both the structure and morphology of the composite nanowires.

Finally, the photocatalytic behaviors of the Ag@TiO_2 anatase core–shell nanowires have been evaluated by observing the degradation of rhodamine B (RhB) dye under visible light illumination at room temperature.§ For comparison, the performances of the TiO_2 anatase nanoparticles and Ag nanowires have also been investigated. As shown in Fig. 4, it can be clearly seen that the Ag@TiO_2 anatase core–shell nanowires exhibit the highest photocatalytic activity and could nearly completely decompose the RhB dye in 15 min. The photodecomposition rate constant k of RhB over Ag@TiO_2 hetero-structures, as calculated from the slopes of ln C_0/C *vs.* time line, is 0.1894 min^{-1}, show much higher degradation rate than the TiO_2 anatase nanoparticles and Ag nanowires (0.0630 min^{-1}, 0.0032 min^{-1}, respectively). Under visible light illumination, the self-sensitization of RhB molecule[35,36] can extend the absorption of TiO_2 into the visible-light region, and the reactions in the whole degradation process for a pure TiO_2 sample are similar to those in dye-sensitized TiO_2 solar cells, that is, RhB molecules transfer photo-excited electrons to TiO_2, while being degraded at the same time. For the Ag@TiO_2 anatase core–shell nanowires, the photon absorption induces a strong localized surface plasmon resonance (LSPR) phenomenon at the Ag@TiO_2 interface, which enhances the generation of electron–positive charges pairs. The electrons generated by the LSPR effect diffuse into the TiO_2 shells, enhancing the generation of $O_2^{\bullet-}$ radicals. Also, the positive charges generated in Ag are used for the generation of $OH^{\bullet}$ radicals. Both $O_2^{\bullet-}$ and $OH^{\bullet}$ radicals play a crucial role in the photocatalytic degradation of organic contaminant molecules.[25,37–39] Therefore, it is clearly demonstrated in the current work that having the core–shell morphology can impart enhancement in the photocatalytic activity. Additionally, neither the photolysis experiment without photocatalyst nor the catalytic experiment without light irradiation showed any observable decrease in RhB concentration with time, demonstrating that photocatalysis was indeed the cause for the decomposition of RhB.

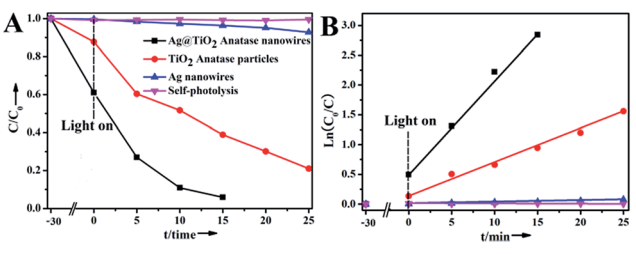

Fig. 4 (A) Photodegradation of RhB without and with the presence of as-prepared Ag@TiO_2 anatase core–shell nanowires, TiO_2 anatase nanoparticles and Ag nanowires under visible light irradiation ($\lambda > 420$ nm) at room temperature; (B) plots of ln(C_0/C) *versus* illumination time representing the fitting using the pseudo-first-order reactions.

Conclusions

We have demonstrated a generic strategy for the successful synthesis of one-dimensional Ag@TiO_2 core–shell nanostructure through hydrolysis reaction and subsequently thermal-induced method. A uniform layer of TiO_2 shell is coated onto the Ag core, thus forming the 1D Ag core@TiO_2 shell semiconductor nanocomposites. Furthermore, the as-achieved Ag@TiO_2 core–shell nanowires exhibit the capability to efficiently catalyze the degradation of organic pollutants with the assistance of photoillumination. This strategy is expected to extend to the synthesis of core–shell nanowires of other inorganic materials such as Ag@SiO_2 core–shell nanowires, Bi@TiO_2 nanostructures, and Bi@SiO_2 nanostructures.

Acknowledgements

This work was supported by the "Hundred Talents Program" of the Chinese Academy of Science and National Natural Science Foundation of China (21273255, 21303232).

Notes and references

‡ Synthesis of Ag@TiO_2 anatase core–shell nanostructures: In a typical synthesis, 3 mL H_2O of Ag nanowires (0.5 g) and PVP (0.04 g) were placed in 200 mL of ethanol under a magnetic stirring rate of 350 rpm. After PVP were completely dissolved, 5 mL ethanol solution of TBT (2.0 g) was injected dropwise with a syringe. The reaction was continued for 30 min and a white dispersion containing Ag@TiO_2 core–shell nanowires was obtained. The product was collected by natural sedimentation, and then the product with water (10 mL) was transferred into a Teflon-lined stainless steel autoclave. The autoclave was kept at 160 °C in an oven for 12 h. After the hydrothermal reaction, the Ag@TiO_2 anatase core–shell sample was obtained. In addition, for comparison, pure TiO_2 amorphous and TiO_2 anatase nanoparticles were synthesized following the above methods in the absence of Ag nanowires.

§ Photocatalytic reactions: In this catalytic activity of experiment, the samples (0.2 g) were put into a solution of RhB dye (100 mL, 4 mg L^{-1}), which was then irradiated with a 300 W Xe arc lamp equipped with an ultraviolet cutoff filter to provide visible light with $\lambda \geq 420$ nm. Before the light was turned on, the solution was stirred in the dark for 30 min to ensure an adsorption/desorption equilibrium between the catalyst and organic dye.

1 M. Hoffmann, S. Martin, W. Choi and D. Bahnemann, *Chem. Rev.*, 1995, **95**, 69.
2 G. Brown, V. Henrich, W. Casey, D. Clark, C. Eggleston, A. Femly, D. Goodman, M. Gratzel, G. Macial, M. McGarthy, K. Nealson, D. Sverjensky, M. Toney and J. Zachara, *Chem. Rev.*, 1999, **99**, 77.

3 W. Yao, X. Xu, H. Wang, J. Zhou, X. Yang, Y. Zhang, S. Shang and B. Huang, *Appl. Catal., B*, 2004, **52**, 109.
4 T. Tong, J. Zhang, B. Tian, F. Chen and D. He, *J. Colloid Interface Sci.*, 2007, **315**, 382.
5 S. Sharma, D. Singh, K. Saini, C. Kant, V. Sharma, S. Jain and C. Sharma, *Appl. Catal., A*, 2006, **314**, 40.
6 W. Wang, J. Zhang, F. Chen, D. He and M. Anpo, *J. Colloid Interface Sci.*, 2008, **323**, 182.
7 J. Chen, M. Yao and X. Wang, *J. Nanopart. Res.*, 2008, **10**, 163.
8 F. Zhang, Y. Pi, J. Cui, Y. Yang, X. Zhang and N. Guan, *J. Phys. Chem. C*, 2007, **111**, 3756.
9 J. Rawat, S. Rana, R. Srivastava, R. Devesh and K. Misra, *Mater. Sci. Eng., C*, 2007, **27**, 540.
10 P. Cozzoli, R. Comparelli, E. Fanizza, M. Curri, A. Agostiano and D. Laub, *J. Am. Chem. Soc.*, 2004, **126**, 3868.
11 S. Standridge, G. Schatz and J. Hupp, *Langmuir*, 2009, **25**, 2596.
12 L. Du, A. Furube, K. Yamamoto, K. Hara, R. Katoh and M. Tachiya, *J. Phys. Chem. C*, 2009, **113**, 6454.
13 K. Awazu, M. Fujimaki, C. Rockstuhl, J. Tominaga, H. Murakami, Y. Ohki, N. Yoshida and T. Watanabe, *J. Am. Chem. Soc.*, 2008, **130**, 1676.
14 Y. Xie, K. Ding, Z. Liu, R. Tao, Z. Sun, H. Zhang and G. An, *J. Am. Chem. Soc.*, 2009, **131**, 6648.
15 K. Matsubara and T. Tatsuma, *Adv. Mater.*, 2007, **19**, 2802.
16 J. Yu, L. Yue, S. Liu, B. Huang and X. Zhang, *J. Colloid Interface Sci.*, 2009, **334**, 58.
17 X. Chen, H. Zhu, J. Zhao, Z. Zheng and X. Gao, *Angew. Chem., Int. Ed.*, 2008, **47**, 5353.
18 H. Chuang and D. Chen, *Nanotechnology*, 2009, **20**, 1.
19 H. Zhang, G. Wang, D. Chen, X. Lv and J. Li, *Chem. Mater.*, 2008, **20**, 6543.
20 T. Hirakawa and P. Kamat, *J. Am. Chem. Soc.*, 2005, **127**, 3928.
21 T. Hirakawa and P. Kamat, *Langmuir*, 2004, **20**, 5645.
22 P. Isabel, D. Koktysh, A. Mamedov, M. Giersig, N. Kotov and L. Liz-Marzán, *Langmuir*, 2000, **16**, 2731.
23 X. H. Yang, H. T. Fu, K. Wong, X. C. Jiang and A. B. Yu, *Nanotechnology*, 2013, **24**, 415601.
24 Y. An, L. Yang, J. Hou, Z. Y. Liu and B. H. Peng, *Opt. Mater.*, 2014, **36**, 1390.
25 H. Eom, J. Y. Jung, Y. Shin, S. Kim, J. H. Choi, E. Lee, J. H. Jeong and I. Park, *Nanoscale*, 2014, **6**, 226.
26 B. Cheng, Y. Le and J. G. Yu, *J. Hazard. Mater.*, 2010, **177**, 971.
27 S. F. Chin, S. C. Pang and F. E. I. Dom, *Mater. Lett.*, 2011, **65**, 2673.
28 J. Du, J. Zhang, Z. Liu, B. Han, T. Jiang and Y. Huang, *Langmuir*, 2006, **22**, 1307.
29 Y. Bi, H. Hu, S. Ouyang, Z. Jiao, G. Lu and J. Ye, *J. Mater. Chem.*, 2012, **22**, 14847.
30 H. Yang and H. Zeng, *J. Phys. Chem. B*, 2004, **108**, 3492.
31 M. Jin, X. Zhang, S. Nishimoto, Z. Liu, D. Tryk, A. Emeline, T. Murakami and A. Fujishima, *J. Phys. Chem. C*, 2007, **111**, 658.
32 Q. Xiang, J. Yu, B. Cheng and H. Ong, *Chem.–Asian J.*, 2010, **5**, 1466.
33 H. Sakai, D. Kanda, H. Shibata, T. Ohkubo and M. Abe, *J. Am. Chem. Soc.*, 2006, **128**, 4944.
34 J. Li and H. C. Zeng, *J. Am. Chem. Soc.*, 2007, **129**, 15839.
35 H. M. Sung-Suh, J. R. Choi, H. J. Hah, S. M. Koo and Y. C. Bae, *J. Photochem. Photobiol., A*, 2004, **163**, 37.
36 T. X. Wu, G. M. Liu, J. C. Zhao, H. Hidaka and N. Serpone, *J. Phys. Chem. B*, 1998, **102**, 5845.
37 F. Wu, X. Y. Hu, J. Fan, E. Z. Liu, T. Sun, L. M. Kang, W. Q. Hou, C. J. Zhu and H. C. Liu, *Plasmonics*, 2012, **8**, 501.
38 Z. K. Zheng, B. B. Huang, X. Y. Qin, X. Y. Zhang, Y. Dai and M. H. Whangbo, *J. Mater. Chem.*, 2011, **21**, 9079.
39 N. Zhou, L. Polavarapu, N. Y. Gao, Y. L. Pan, P. Y. Yuan, Q. Wang and Q. H. Xu, *Nanoscale*, 2013, **5**, 4236.